Determination of Parameters Affecting Transport in Polymeric Membranes: Parallels between Pervaporation and Nanofiltration

Bart Van der Bruggen,*,†,‡ Johannes C. Jansen*,‡ Alberto Figoli,*,‡ Jeroen Geens,† Dimitri Van Baelen,† Enrico Drioli,‡ and Carlo Vandecasteele†

University of Leuven, Department of Chemical Engineering, Laboratory for Applied Physical Chemistry and Environmental Technology, W. de Croylaan 46, B − 3001 Heverlee, Belgium and Research Institute on Membrane Technology (ITM-CNR), c/o University of Calabria, via P. Bucci, cubo 17/C, 87030 Rende (Cosenza), Italy

Received: April 22, 2004; In Final Form: June 29, 2004

The differences in structure and transport mechanisms of nanofiltration (NF) and pervaporation (PV) membranes were studied by measuring (a) water and ethanol fluxes and raffinose rejections obtained during nanofiltration with two NF membranes (Desal 5 DK and MPF 50) and two PV membranes (PV 2201 and PV 1070); (b) water and ethanol fluxes and water/ethanol-*n*-propanol separation factors obtained during pervaporation with the same membrane sequence; and (c) gas and vapor (water, ethanol) permeance with the same membrane sequence. In the nanofiltration experiments, it was observed that transport is determined by hydrophilicity/hydrophobicity of the membrane, the presence of pores and their geometry, membrane thickness, and solvent properties. Pervaporation experiments confirmed the nanoporosity of the NF membranes; a comparison of fluxes showed that transport in pervaporation is thought to depend on preferential sorption. Gas permeance measurements with inert gases provided clear evidence for the porous nature of NF Desal 5 DK and the dense nature of PV 1070; PV 2201 was found to be porous. However, this membrane swells significantly when brought in contact with water or ethanol vapors, rendering a dense membrane suitable for pervaporation. For the other membranes, swelling was also observed, together with plasticization of the polymers.

Introduction

Nanofiltration and pervaporation are both membrane processes in which diffusion may contribute significantly to the transport of components from the feed side to the permeate side.[1−5] Pervaporation membranes are dense; therefore, it is generally accepted that transport exclusively takes place by a mechanism of preferential sorption into the membrane polymer, followed by diffusive transport through the membrane phase.[1] Separation occurs as a result of differences in sorption/diffusion behavior between components in the feed mixture. Hydrophilic membranes can be used for dehydration of organic solvents, because water readily sorbs into the hydrophilic polymer material, whereas the organic solvent remains in the feed solution. The separation factor, defined as the enrichment of a component in the permeate phase compared to the feed phase, relative to a reference component, reflects the process efficiency. Separation factors obtained with commercial hydrophilic pervaporation membranes allowed a cost-effective industrial application of solvent dehydration; as a consequence, pervaporation has become a reliable standard method.[6−8]

For both hydrophobic and hydrophilic pervaporation, the sorption−diffusion transport mechanism can be described by readily available sorption−diffusion models originating from the description of transport through reverse osmosis membranes.[14] All of these models are essentially based on a generalization of Fick's law for diffusion but range in complexity by taking different nonidealities into account.[15] Multicomponent diffusion can be taken into account by using the Stefan−Maxwell equation[16] in combination with a sorption calculation using, for example, UNIQUAC[17,18] or modifications of the Flory−Huggins model.[19] The influence of the free volume of the polymer is described by molecular dynamics or by model adaptations.[20−22] Furthermore, interactions between components and the membrane by plasticization can also be taken into account,[23,24] and the mass transfer resistance originating from concentration polarization and the porous support can be estimated.[25,26]

Despite these widely accepted modeling efforts, they may lead to erroneous assumptions for membranes with a larger free volume or nanoporous membranes.[27] The permeation flux is the sum of a bulk flux and a diffusional flux, with the bulk flux being negligible for dense pervaporation membranes. However, the bulk flux may contribute significantly to the total permeate flux for nanoporous membranes; application of sorption−diffusion models, even with the adaptations described above, then leads to misinterpretations and wrong predictions. This might be an explanation for deviations found with multicomponent mixtures, when the permeation flux of one of the permeant is much higher than the others, and it also explains why sorption−diffusion models are essentially not valid for nanoporous membranes. On the other hand, swelling may cause a shift in the ratio of bulk flux and diffusive flux so that membrane transport shifts from porous flow to diffusive transport. Similar to pervaporation, the solvent flux in nanofiltration of organic solvents seems to be governed by hydrophilicity or hydrophobicity of the membranes,[28,29] which is a

* Address correspondence to these authors. Van der Bruggen: tel.: +32 16 32.23.40; fax: +32 16 32.29.91; e-mail: bart.vanderbruggen@cit.kuleuven.ac.be. Jansen and Figoli: tel.: +39 0984 49.20.14; fax: +39 0984 40.21.03; e-mail: jc.jansen@itm.cnr.it and a.figoli@itm.cnr.it.

† University of Leuven.

‡ Research Institute on Membrane Technology.

10.1021/jp048249g CCC: $27.50 © 2004 American Chemical Society
Published on Web 08/11/2004

qualitative confirmation of a sorption−diffusion mechanism. A quantitative description, however, should take a combined convection−diffusion mechanism into account.[30] This method works relatively well if only aqueous solutions are used and leads to several models describing fluxes and rejections in nanofiltration.[31−33] Some models are based on solution diffusion,[34] while others assume that separations are based on sterically hindered transport through nanopores.[35,36] Both approaches have a fairly good predictive value, which may be a little surprising because they reflect a different transport mechanism and a different membrane structure. When organic solvents are considered, differences in the swelling behavior further complicate the interpretation of the transport mechanism, because the ratio of bulk flux and diffusive flux may shift because of membrane swelling. Therefore, insight in the relative importance of diffusive transport on fluxes and separations in nanofiltration with organic solvents is still limited.

In this article, transport in (dense) pervaporation membranes and (nanoporous) nanofiltration membranes is compared, both in the pervaporation and the nanofiltration process. Hence, in both membrane processes similar transport mechanisms may occur, such as diffusion, and NF membranes might thus show PV properties and vice versa. The objective is to use the knowledge of transport mechanisms in pervaporation to estimate the relative importance of diffusion in nanofiltration membranes, which have a larger free volume. The methods used in the comparison are based on (a) performance measurements in pervaporation and nanofiltration and (b) investigation of the characteristics of the membrane materials influencing the membrane performance. Gas and vapor permeation measurements are carried out to get supporting information on the membrane structure under dry conditions or conditions of low to medium liquid activity.

Materials and Methods

Nanofiltration Experiments. Nanofiltration (NF) experiments were carried out with a solvent compatible laboratory unit. A cross-flow filtration cell containing flat sheet membranes with a diameter of 2.27 cm and an effective surface area of 4.05 cm^2 was used. The transmembrane pressure ranged from 7 to 45 bar, depending on the permeability of the membranes. Fluxes are in principle proportional to pressure, although friction losses result in fluxes lower than expected at high pressures. Two NF membranes (NF MPF 50, Koch—hydrophobic, and NF Desal 5 DK, Osmonics—hydrophilic) and two PV membranes (PV 1070, Sulzer—hydrophobic, and PV 2201, Sulzer—hydrophilic) were used for nanofiltration. MPF-50 consists of three layers, with a backing made of a polypropylene−polyethylene blend. The polymeric layer and the top polymeric layer are a proprietary polymer (synthesized by Koch) and are silicone based. The top layer of Desal 5 DK is a cross-linked aromatic polyamide. PV 2201 is made of PVA; PV 1070 is a (zeolite-filled) PDMS membrane. Fluxes were measured for water, ethanol, and a 50:50 vol % mixture of water and ethanol. In each solvent, the rejection was measured for raffinose (MW 504, feed concentration 100 mg/l). Raffinose concentrations in the feed and permeate fractions were determined by spectrophotometry after reaction with phenol in sulfuric acid. In this way, by using uncharged components, the influence of surface charges for the NF membranes is avoided.

The flow and transmembrane pressure are set manually by means of the valves in the feed pipe and in the bypass. The retentate is recycled to the feed tank; the permeate can be recycled as well; samples can be taken at any time in the experiment. No significant concentration changes took place during the experiment. The temperature in all experiments was 25 °C. A cooling coil inside the feed tank was used to compensate for the temperature increase caused by the pump, so that the temperature could automatically be kept stable at a preset value.

For dense membranes, the solvent flux J ($m^3 \cdot m^{-2} \cdot s^{-1}$) can be described as

$$J = \frac{D_s c_s V_s}{RT\rho\Delta x}(\Delta P - \sigma \cdot \Delta\pi) \tag{1}$$

where D_s is the diffusion coefficient of the solvent in the membrane ($m^2 \cdot s^{-1}$), c_s is the concentration of the solvent in the membrane ($kg \cdot m^{-3}$), V_s is the molar volume ($m^3 \cdot mole^{-1}$), R is the gas constant ($J \cdot mole^{-1} \cdot K^{-1}$), T is the absolute temperature (K), ρ is the solvent density ($kg \cdot m^{-3}$), and Δx is the membrane thickness (m); ΔP is the pressure difference (Pa), $\Delta\pi$ is the osmotic pressure difference (Pa), and σ is the reflection coefficient (−), representing the percentage rejection of components contributing to the osmotic pressure.

For porous membranes, the Hagen−Poiseuille equation can be used for the solvent flux J ($m^3 \cdot m^{-2} \cdot s^{-1}$):

$$J = \frac{\epsilon \cdot r^2}{8\eta\tau}\frac{\Delta P}{\Delta x} \tag{2}$$

where ϵ is the surface porosity (−), r is the pore size (m), η is the viscosity (Pa·s), τ is the tortuosity (−), ΔP is the applied pressure difference (Pa), and Δx is the membrane thickness (m). Only the open, communicating pores must be considered in the surface porosity. In a relatively dense material, where the resistance of the bulk cannot be ignored, the overall porosity should be taken into account.

Flux and rejection values are an average of at least three measurements with the same membrane sheet; flux measurements were carried out repeatedly (three times or more) for different membranes of the same type.

Pervaporation Experiments. All pervaporation (PV) experiments were carried out with a laboratory test cell (Lab Test Cell Unit, Sulzer Chemtech). The feed is heated in a 3 L stainless steel container and kept at constant temperature of 50 °C by a temperature control unit. A centrifugal pump circulates the feed. The membrane module contains a circular flat sheet membrane with a diameter of 6 in. (152.4 mm). The permeate is collected in a glass container, cooled in a Dewar flask with liquid nitrogen. The vacuum is maintained by a two-stage vacuum pump.

The same membranes as used in the NF experiments were also used for pervaporation (i.e., two NF membranes and two PV membranes). Fluxes were measured for water, ethanol, and a water/ethanol mixture, to which 10 vol % of *n*-propanol was added. The equation for the flux J per unit of membrane surface area ($m^3 \cdot m^{-2} \cdot s^{-1}$) in pervaporation was

$$J = \frac{D_i \cdot S_i}{\Delta x}\Delta p_i \tag{3}$$

where D_i is the diffusion coeeficient of the component in the membrane ($m^2 \cdot s^{-1}$), S_i is the solubility coefficient of the component in the membrane ($m^3 \cdot m^{-3} \cdot Pa^{1-}$), Δx is the membrane thickness (m), and Δp_i is the difference in vapor pressure (Pa).

For the evaluation of the separation achieved with a given membrane, the separation of *n*-propanol from the feed solution

TABLE 1: Total Permeability (l/m² h bar) of the Four Membranes Used under NF Conditions: (1) at 7 bar; (2) at 30 bar; (3) at 45 bar

membrane	nature	water	water:ethanol 50:50	ethanol
PV 1070	hydrophobic	0.08(3)	<0.06	<0.06
PV 2201	hydrophilic	0.08(1)	<0.06	0.07(1)
NF MPF 50	hydrophobic	0.23(2)	1.3(1)	5.2(1)
NF Desal 5 DK	hydrophilic	2.5(1)	1.4(1)	1.7(1)

was evaluated. The concentration of *n*-propanol in the feed and permeate fractions was measured by gas chromatography. No significant concentration changes took place in the feed solution during the PV experiment. Flux and rejection values are an average of at least three measurements with the same membrane sheet; flux measurements were carried out repeatedly (three times or more) for different membranes of the same type.

Gas and Vapor Permeance Measurements. The pure gas and vapor permeance of the membranes was measured on a testing instrument constructed by GKSS Forschung, Germany. The instrument consists of a thermostated membrane cell with fixed permeate volume at the feed side connected via a series of control valves to different gas flasks. The procedure is based on a pressure increase measurement on the fixed volume permeate side of the membrane cell, which is completely evacuated before the start of the measurement. The feed side of the membrane is maintained at atmospheric pressure for gases or at a pressure below the vapor pressure for vapors. The permeability is defined as the volume (m^3 STP) permeating through a defined membrane surface area (m^2) per time unit (h) and per unit of pressure difference (bar). In a steady-state permeation experiment, the permeability can be calculated as

$$L = \frac{22.41V^*3600}{R\cdot T\cdot A\cdot t}\ln\left(\frac{p_F - p_0}{p_F - p_{P(t)}}\right)\left(\text{in}\ \frac{m^3{}_N(\text{STP})}{m^2\,\text{h bar}}\right) \quad (4)$$

where V is the permeate volume (m^3), $R = 0.08314$ m^3 bar·kmol^{-1} K^{-1}, T is the temperature (K), A is the membrane surface area (m^2), t is the measured time (s), p_F is the feed pressure (Pa), p_0 is the initial permeate pressure (Pa), $p_{P(t)}$ is the permeate pressure at time t (Pa), 3600 is a conversion factor (s/h), and 22.41 is the molar volume (m^3 N/kmol). Applied gases were He, CH_4, N_2, O_2, and CO_2; vapors used were water (pressure range 0−25 mbar at 25 °C and 0−105 mbar at 50 °C) and ethanol (pressure range 0−80 mbar at 25 °C).

Results and Discussion

Nanofiltration Permeability. The permeabilities obtained for nanofiltration with NF membranes and PV membranes are summarized in Table 1. For the PV membranes a very low permeability was obtained, in particular for the hydrophobic PV 1070 membrane. The hydrophobic NF MPF 50 membrane had a very low water permeability, while the permeability for ethanol, which is less polar, was much larger. For the hydrophilic membranes, this trend is reversed in pure liquids: permeability of the less polar ethanol is lower than that of water. Thus, the hydrophobicity/hydrophilicity of the membrane is a factor determining the permeability in nanofiltration, for PV as well as for NF membranes. However, other factors such as the feed viscosity also play a role; flux is generally inversely proportional to viscosity. The viscosity of the 50/50 v/v mixture is larger than that of pure water or pure ethanol; this results in a lower permeability than for each of the pure liquids for the hydrophilic membranes. For the hydrophobic NF MPF 50 membrane, the hydrophobicity effect is dominant.

The parameters that may explain the difference between NF membranes and PV membranes are given by the flux equations for dense and for porous membranes. Because the experimental conditions are comparable for NF and PV membranes, the membrane parameters responsible for the differences in transport properties are the membrane thickness Δx, the diffusion coefficient of the solvent inside the membrane D_s, or the presence of pores in the membrane structure, reflected by the combination $\epsilon\, r^2/\tau$. The thickness of the separating layer of the membranes is shown on SEM images (Figure 1). The top layer of the NF membranes is ca. 1 μm; the top layer of the PV 2201 membrane is ca. 2 μm, whereas PV 1070 apparently has a thicker top layer; the structure of the latter membrane is rather granular. Differences in membrane thickness may only partly explain the experimental results in Table 1. Fluxes obtained with PV 1070 are small or not detectable, which might be attributed to the thick top layer. The top layer of PV 2201 is somewhat thicker than that of the NF membranes, but the flux for the NF membranes are 1 to 2 orders of magnitude larger, much more than could be expected from the thickness of the top layer. However, membrane thickness and hydrophilicity might not be the only mechanisms determining the solvent flux. Apparently, there is another difference between NF and PV, given the larger fluxes, for example, for Desal 5 DK compared to PV 2201 (both hydrophilic). The NF membranes might have larger diffusion constants for permeating solvents/solutes, caused by a difference in swelling behavior, which results in a larger mobility of polymeric chains, and causes higher fluxes if the membrane is considered dense. Additionally, the NF membranes may have a more open structure; the free volume between the polymeric chains then becomes a network of nanovoids.

It will be shown in the gas permeation measurements below that in dry conditions the NF membranes are clearly (nano)-porous. The lack of selectivity of the NF membranes in PV experiments (see next section) suggests that the same is true under wet conditions. Otherwise, if the polymer matrix shows very strong swelling by the solvent, the pores may be squeezed and a more or less dense (hydro)gel may be formed, which is also characterized by very high permeabilities. However, such structures should have at least some degree of permselectivity for water and alcohols, in contrast to what is observed in the PV experiments (below). Therefore, the nanoporous structure is believed to exist both in the wet state and in the dry state.

Nanofiltration Selectivity. Raffinose rejections measured with NF membranes are given in Table 2. For the PV membranes, it was not possible to measure rejections with sufficient accuracy, given the small permeate fluxes.

For the NF membranes, the rejection depends strongly on the pore size of the membrane. NF Desal 5 DK has a molecular weight cutoff (MWC) of ca. 150−300, while the MWC of NF MPF 50 is ca. 700 (values indicated by manufacturers). This explains the low rejections for NF MPF 50. Furthermore, the hydrophobicity/hydrophilicity of the membrane also plays a role, as can be seen from the data of Desal 5 DK. With decreasing solvent polarity, the rejection decreases from 99% with pure water to 20% with pure ethanol, while the overall permeance changes to a much less extent. The two NF membranes have exactly the opposite behavior in their permeability and selectivity. MPF 50 has a minimum in the rejection for the solvent mixture, while Desal 5 DK has a gradually decreasing rejection with decreasing solvent polarity. These differences in rejections for different solvents can be explained by assuming solvation of the membrane pores. The hydrophilic Desal 5 DK membrane shows less pore solvation for less polar solvents; the available

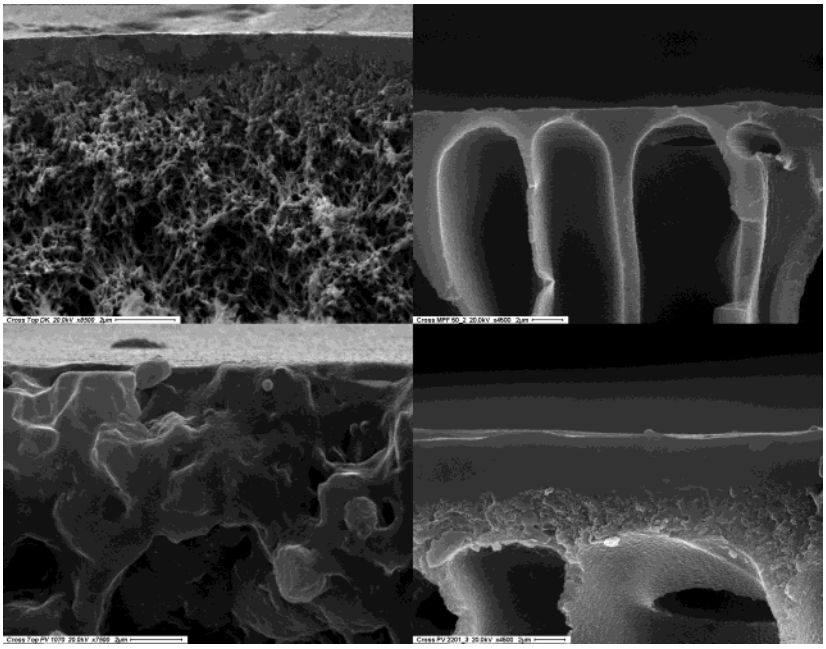

Figure 1. SEM images of the cross section of NF Desal 5 DK (upper left, scale 2 μm), MPF 50 (upper right, scale 2 μm), PV 1070 (lower left, scale 2 μm), and PV2201 (lower right, scale 2 μm).

TABLE 2: NF Rejection (%) of Raffinose (MW 504) in Water, 50/50 Vol % Water/Ethanol, and Ethanol[a]

	water	water:ethanol 50:50	ethanol
PV 1070	n.m.	n.m.	n.m.
PV 2201	n.m.	n.m.	n.m.
NF MPF 50	37	12	30
NF Desal 5 DK	99	85	20

[a] n.m.: not measurable.

TABLE 3: Total Flux in Pervaporation Experiments (T = 70 °C) in l/m^2 h (10% *n*-Propanol Added)

	water	water:ethanol 50:50	ethanol
PV 1070	0.27	0.66	1.2
PV 2201	7.5	2.3	0.56
NF MPF 50	9.4	11.7	14.7
NF Desal 5 DK	21.6	17.2	10.3

pore opening for solute permeation is thus larger (lower rejections). Pores of MPF 50 show more solvation for less polar solvents, but in this case there is also an effect of hydration of the (polar) solute. Both effects are in the opposite direction, resulting in an intermediate minimum.

Thus, it can be concluded that the NF membranes have pores, even though they are on the interface of porous membranes (convective transport or surface diffusion) and dense membranes (bulk diffusion).

Pervaporation Permeability. Fluxes and separation factors obtained in pervaporation experiments are given in Tables 3 and 4. Similar to the nanofiltration experiments, the influence of hydrophobicity/hydrophilicity is obvious, given the differences in fluxes for the hydrophobic PV membrane and the hydrophilic PV membrane; to a lesser extent, the same observation was made for the hydrophobic and the hydrophilic NF membrane. In this case, it is thought that fluxes are (partly) determined by sorption of the permeating components. The sorption step consists of dissolution of a component and swelling of the polymer matrix; because this heavily depends on hydrophobicity/hydrophilicity differences between components and the polymer, the contribution of sorption in the overall transport should lead to a difference in fluxes depending on the hydrophobicity/hydrophilicity of the membrane. This was clearly observed in the experiments; it can be concluded that there is a large contribution of sorption to the overall transport.

TABLE 4: Separation Factor eq 7[a] in a Pervaporation Experiment

	water + *n*PrOH	water:ethanol 50:50 + *n*PrOH	ethanol + *n*PrOH
PV 1070	11.3	1.3	0.76
PV 2201	0.33	0.059	0.23
NF MPF 50	1.1	1.0	1.0
NF Desal 5 DK	0.76	0.88	0.82

[a] The subscripts p and f refer to the permeate and feed, respectively. T = 70 °C.

For the NF membranes, where convective transport or surface diffusion is dominant, transport can be faster so that fluxes are considerably higher.

Pervaporation Selectivity. Table 4 summarizes the separation factors obtained in the PV experiments, calculated as

$$\alpha = \frac{c_{p,n-prop}}{c_{p,water+ethanol}} \cdot \frac{c_{f,water+ethanol}}{c_{f,n-prop}} \quad (5)$$

where subscripts p and f refer to the permeate and feed, respectively. For PV 1070, the separation factor decreases when water is replaced by ethanol. In the absence of ethanol (slightly more polar but smaller than *n*-propanol, resulting in a slight preference of ethanol transport), the separation factor is (much) larger than 1; concurrence with ethanol leads to a separation factor even below 1 (preferential transport of ethanol). For PV 2201, preferential transport of water occurs. The larger the "organic" (ethanol + *n*-propanol) fraction, the more pronounced this is. However, for the 90% ethanol mixture, no water is present; preferential ethanol tranpsort takes place, but the separation is worse than for water (closer to 1). This corresponds to the effect of partial pressure on selectivity in pervaporation: the smaller the partial pressure of preferentially permeating component in the feed is, the larger the selectivity.

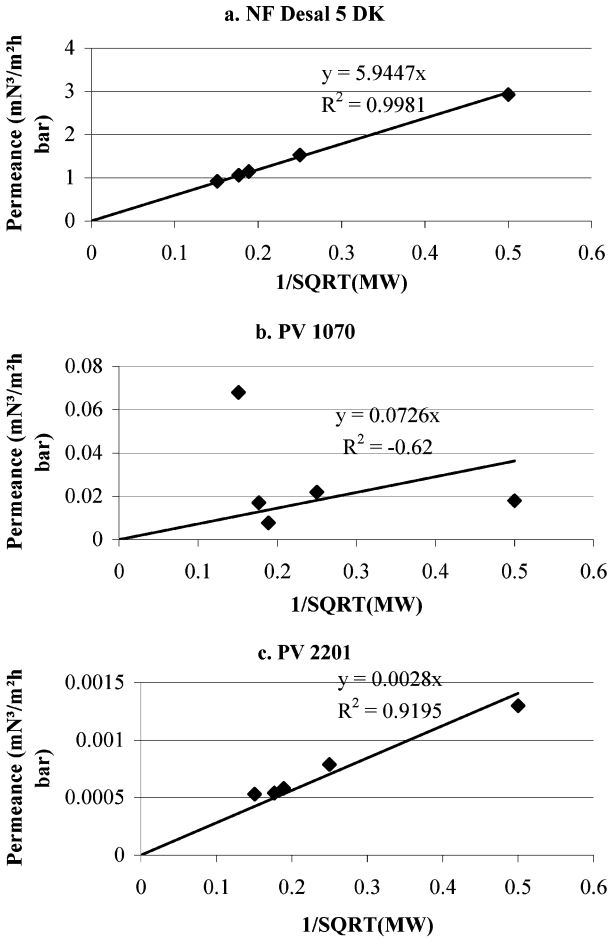

Figure 2. Gas permeance vs $MW^{-0.5}$ for the NF and PV membranes. Applied gases were He, CH_4, N_2, O_2, and CO_2; temperature was 25 °C.

TABLE 5: Pure Gas Permeance for the PV and NF Membranes ($mN^3/m^2 \cdot h \cdot bar$)

	NF Desal 5 DK	PV 1070	PV 2201
O_2	1.06	0.017	0.00054
N_2	1.15	0.0077	0.00058
methane	1.53	0.022	0.00079
helium	2.93	0.018	0.0013
CO_2	0.92	0.068	0.00053

No separation was obtained using the NF MPF 50 membrane. Surprisingly, a slight separation was obtained using the NF Desal 5 DK membrane: transport of *n*-propanol, the largest and most apolar component, is slower than for water or ethanol. Separation factors were below 1 and nearly constant over the whole concentration range. The separation might be a result of size exclusion, although *n*-propanol is much smaller than the MWCO of the membrane. Additionally, sorption in the bulk material (determined by differences in hydrophilicity) may also play a role in the separation: less *n*-propanol sorbs in the bulk of the membrane, resulting in a somewhat lower concentration in the permeate. Thus, even though the NF membranes are porous, the dense bulk material may also add somewhat to solvent and solute transport.

Gas Permeability. Gas permeances for the NF and PV membranes are summarized in Table 5 and Figure 2. No gas permeation measurements could be carried out on the NF MPF 50 membrane, which is stored in a water/ethanol mixture to preserve the highly swollen state of the top layer. The vacuum applied during the gas permeation measurements leads to deswelling and crack formation in the top layer. Gas permeances of the other NF membrane (Desal 5 DK) were 2 to 3 orders of magnitude larger than those for the PV membranes PV 1070 and PV 2201, which supports the earlier assumption that NF Desal 5 DK is not a dense membrane. Moreover, in the pervaporation experiments the difference in fluxes between the PV and NF membranes was also approximately 2 orders of magnitude. In the nanofiltration experiments, where transport occurred completely in the liquid phase, the differences were smaller.

The gas permeation measurements were further used to verify the pore structure of the different membranes. For very large pores, where contact with the pore wall is negligible and viscous flow occurs through the pores, the differences in pure gas flux depend on the gas viscosity and no significant separation is obtained. For smaller pores, when the free path length of the permeant molecules is of the same order as the pore size, Knudsen diffusion occurs. In this case, the permeance can be described by (adapted from 1)

$$J = \frac{V_s \cdot D_k \cdot \Delta p}{R \cdot T \cdot \tau \cdot l}, \text{ with } D_k = 0.66 r \sqrt{\frac{8RT}{\pi MW}} \qquad (6)$$

T and MW are the temperature (K) and molecular weight (−), respectively, J is the flux ($m^2 \cdot m^{-3} \cdot s^{-1}$), R is the ideal gas constant ($J \cdot mole^{-1} \cdot K^{-1}$), V_s is the molar volume ($m^3 \cdot mole^{-1}$), l is the path length (m), D_i is the diffusion coefficient of component i ($m^2 \cdot s^{-1}$), and Δp is the vapor pressure difference (Pa). Thus, permeance is inversely proportional to the square root of the penetrant's molecular weight. From Table 5, it can be seen that all membranes exhibit, at least to some extent, a pure gas selectivity. In Figure 2, the gas permeance is given as a function of the inverse square root of the molecular weight of the gases used. For NF Desal 5 DK, Knudsen diffusion clearly occurs ($r^2 = 0.998$), which confirms the (nano)porous nature of the membrane. For PV 1070, Knudsen diffusion does not occur; in particular, the CO_2 permeance is much higher and the helium permeance lower than the expected trend for Knudsen diffusion. The observed selectivities are typical for PDMS, confirming that this membrane has a dense active layer of PDMS in which transport is controlled by the solution−diffusion mechanism. From literature values of the PDMS permeability, for example, $P(CO_2) = 3200$ Barrer,[1] the effective thickness of the active layer of the PV 1070 membrane (permeance = 0.068 $m^3/(m^2\ h\ bar)$) can be calculated as 127 micron. This value is much higher than the real thickness of the top layer and indicates that the support layer on which PDMS is deposited has a low surface porosity. Gas permeance through PV 2201 is very low, much lower than that of NF Desal 5 DK and PV 1070. The relative permeances of the different gases are nearly according to the Knudsen equation, with a slightly higher CO_2 flux and a slightly lower helium flux than expected (correlation $r^2 = 0.919$). This indicates that the membrane is nanoporous under these conditions and that Knudsen diffusion is the dominating mechanism, while at the same time a minor fraction of the total flux is due to the solution−diffusion mechanism, apparently through the dense fraction of the membrane surface.

These results of the gas permeation through PV 2201 are interesting as they are in contrast with the results of the nanofiltration and pervaporation measurements, where the high selectivity of this membrane was clearly demonstrated. This is only possible when the active layer is dense. Apparently, during PV and NF experiments, the direct contact of the membrane with the liquid phase causes swelling of the polymer, which, in turn, causes complete squeezing of the nanopores. Water

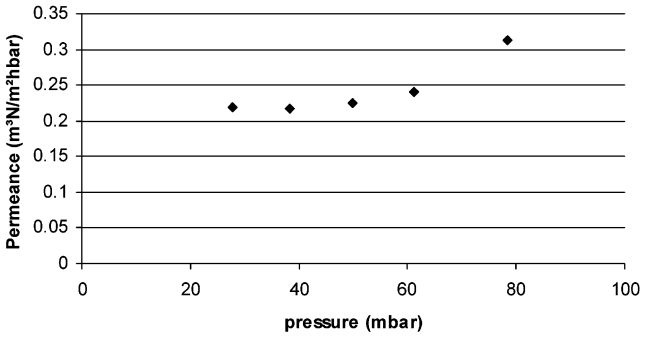

Figure 3. Ethanol vapor permeance as a function of the feed pressure for NF Desal 5 DK (temperature: 25 °C, permeate pressure increase 8−13 mbar).

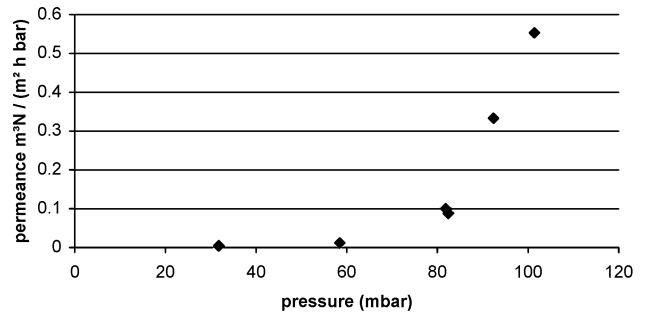

Figure 4. Water vapor permeance for PV 2201 as a function of the feed pressure (temperature: 50 °C, permeate pressure increase 0 to max 12 mbar).

permeability in this swollen state was orders of magnitude higher than the gas permeance of a molecule with the same molar mass (methane), emphasizing the large solution−diffusion contribution.

By measuring gas permeabilities, the dry membrane structure was studied without any interaction effects that may occur during contact with a liquid feed solution, as in pervaporation or nanofiltration. An intermediate step between gases and liquids that is considered here is the measurement of vapor permeances, using water and ethanol vapors.

Figure 3 gives the equilibrium permeance of ethanol vapor as a function of the applied pressure for the NF Desal 5 DK membrane; only a slight increase can be observed at the highest vapor pressures. This probably indicates that surface transport of the condensed vapor along the membrane pore surface plays an increasingly important role at higher vapor pressures. Changes in the degree of swelling of the polymer matrix by the vapor are probably negligible (on this time scale) as this would lead to a squeezing of the pores and a reduction of the permeance with time. The absolute value of the ethanol permeance is much lower than one would expect for Knudsen diffusion of a molecule with this molecular weight (see Figure 2a—inverse square root of the molecular weight is 0.147, from which an expected value of approximately 0.88 can be calculated), probably because of gas-phase interactions or interactions with the pore walls of this clearly nonideal gas.

The water vapor permeance as a function of the applied pressure is given in Figure 4 for PV 2201, a membrane found to be nanoporous during gas permeation measurements. From Figure 4, it can be seen that the permeance at low pressures is low, similar to gas permeances. At elevated pressures, however, the permeance rapidly increases, much more than one would expect on the basis of a contribution of surface diffusion. This behavior is unlikely for a porous material and can only be explained when assuming that the pores become closed when the membrane material swells, thus converting the nanoporous membrane into a dense membrane suitable for pervaporation. Indeed, in the pervaporation measurements described above, it was found that this membrane behaves as a dense permselective membrane. The further increase of the permeance with increasing pressure of the water vapor can be explained by the further swelling and strong plasticization of the polymer matrix (poly(vinyl alcohol)) upon contact with higher water vapor pressures at the feed side. The higher degree of swelling, and thus the higher water concentration in the polymer, together with the increased mobility of the polymer chains increase the water permeance of the membrane.

Conclusions

The morphology of polymeric PV and NF membranes has been studied directly by SEM and indirectly by their transport properties. The nature of the membranes depended on the experimental conditions. For example, the PV membranes studied are dense or they may be nanoporous and become dense upon contact with liquids or vapors. The NF membranes should be characterized as nanoporous materials; however, similarly to the PV membranes, swelling may shift the NF membrane structure to a more dense material. The membrane properties (such as hydrophobicity/hydrophilicity, membrane thickness, pore dimensions) as well as solvent properties (polarity, molar volume, viscosity) affect swelling; thus, the membrane structure may differ from application to application. These considerations even leave the possibility of obtaining a dense NF membrane.

Under the normal operating conditions, transport through the dense PV membranes occurs entirely by solution diffusion, where the limiting step is the diffusion through the membrane top layer. However, if the active layer consists of a strongly swelling polymer (e.g., poly(vinyl alcohol) in PV 2201), gas transport under dry conditions may be dominated by Knudsen diffusion because of the nanoporous nature of the polymer film. Thus, a membrane does not necessarily need to be dense to be a good PV membrane, but in operation conditions it must become dense. Transport through NF membranes is governed by pore flow, possibly influenced by solvatation of membrane pores.

Changes of the nature of the membrane under different conditions offer the perspective of using the same membrane for different types of separation processes.

$$\alpha = \frac{c_{\mathrm{p},n-\mathrm{prop}}}{c_{\mathrm{p,water+ethanol}}} \cdot \frac{c_{\mathrm{f,water+ethanol}}}{c_{\mathrm{f},n-\mathrm{prop}}} \tag{7}$$

Acknowledgment. This study was carried out with an FWO-Vlaanderen postdoctoral grant for B. Van der Bruggen.

References and Notes

(1) Mulder, M. *Basic Principles of Membrane Technology*, 2nd ed.; Kluwer Academic: Dordrecht, The Netherlands, 1996.

(2) Wijmans, J. G.; Baker, R. W. The solution-diffusion model: a review. *J. Membr. Sci.* **1995**, *107*, 1−21.

(3) White, L. S. Transport properties of a polyimide solvent resistant nanofiltration membrane. *J. Membr. Sci.* **2002**, *205* (1−2), 191−202.

(4) George, S. C.; Thomas, S. Transport phenomena through polymeric systems. *Prog. Polym. Sci.* **2001**, *26* (6), 985−1017.

(5) Mulder, M. H. V.; Smolders, C. A. Mass-transport phenomena in pervaporation processes. *Sep. Sci. Technol.* **1991**, *26* (1), 85−95.

(6) Jiraratananon, R.; Chanachai, A.; Huang, R. Y. M.; Uttapap, D. Pervaporation dehydration of ethanol−water mixtures with chitosan/hydroxyethylcellulose (CS/HEC) composite membranes I. Effect of operating conditions. *J. Membr. Sci.* **2002**, *195* (2), 143−151.

(7) Huang, R. Y. M.; Pal, R.; Moon, G. Y. Pervaporation dehydration of aqueous ethanol and isopropanol mixtures through alginate/chitosan two

ply composite membranes supported by poly(vinylidene fluoride) porous membrane. *J. Membr. Sci.* **2000**, *167* (2), 275−289.

(8) Burshe, M. C.; Sawant, S. B.; Joshi, J. B.; Pangarkar, V. G. Dehydration of ethylene glycol by pervaporation using hydrophilic IPNs of PVA, PAA and PAAM membranes. *Sep. Purif. Technol.* **1998**, *13* (1), 47−56.

(9) Lipnizki, F.; Hausmanns, S.; Ten, P. K.; Field, R. W.; Laufenberg, G. Organophilic pervaporation: prospects and performance. *Chem. Eng. J.* **1999**, *73* (2), 113−129.

(10) Dotremont, C.; Goethaert, S.; Vandecasteele, C. Pervaporation behavior of chlorinated hydrocarbons through organophilic membranes. *Desalination* **1993**, *91* (2), 177−186.

(11) Athayde, A. L.; Baker, R. W.; Daniels, R.; Le, M. H.; Ly, J. H. Pervaporation for wastewater treatment. *Chemtech* **1997**, *27* (1), 34−3.

(12) Lipnizki, F.; Field, R. W.; Ten, P. K. Pervaporation-based hybrid process: a review of process design, applications and economics. *J. Membr. Sci.* **1999**, *153* (2), 183−210.

(13) David, M.-O.; Gref, R.; Nguyen, T. Q.; Neel, J. Pervaporation-esterification coupling: Part 1: Basic kinetic model. *Chem. Eng. Res. Des.* **1991**, *69* (4), 335−340.

(14) Lee, C. H. Theory of reverse-osmosis and some other membrane permeation operations. *J. Appl. Polm. Sci.* **1975**, *19*, 83−95.

(15) Lipnizki, F.; Tragardh, G. Modelling of pervaporation: Models to analyze and predict the mass transport in pervaporation. *Sep. Purif. Methods* **2001**, *30* (1), 49−125.

(16) Schaetzel, P.; Vauclair, C.; Luo, G.; Nguyen, Q. T. The solution-diffusion model - Order of magnitude calculation of coupling between the fluxes in pervaporation. *J. Membr. Sci.* **2001**, *91* (1−2), 103−108.

(17) Bausa, J.; Marquardt, W. Detailed modeling of stationary and transient mass transfer across pervaporation membranes. *AIChE J.* **2001**, *47* (6), 1318−1332.

(18) Heintz, A.; Stephan, W. A generalized solution diffusion-model of the pervaporation process through composite membranes 1. Prediction of mixture solubilities in the dense active layer using the UNIQUAC model. *J. Membr. Sci.* **1994**, *89* (1−2), 143−151.

(19) Ghoreyshi, S. A. A.; Farhadpour, F. A.; Soltanieh, M. Multicomponent transport across nonporous polymeric membranes. *Desalination* **2002**, *144* (1−3), 93−101.

(20) Hofmann, D.; Fritz, L.; Ulbrich, J.; Schepers, C.; Bohning, M. Detailed-atomistic molecular modeling of small molecule diffusion and solution processes in polymeric membrane materials. *Macromol. Theory Simul.* **2000**, *9* (6), 293−327.

(21) Wang, B. G.; Yamaguchi, T.; Nakao, S. Prediction of solvent solubility, diffusivity and permeability in glassy polymeric membranes. *Polymer* **2001**, *42* (12), 5225−5232.

(22) Chen, C. X.; Han, B. B.; Li, J. D.; Shang, T. G.; Zou, J.; Jiang, W. J. A new model on the diffusion of small molecule penetrants in dense polymer membranes. *J. Membr. Sci.* **2001**, *187* (1−2), 109−118.

(23) Shieh, J. J.; Huang, R. Y. M. A pseudophase-change solution-diffusion model for pervaporation. I. Single component permeation. *Sep. Sci. Technol.* **1998**, *33* (6), 767−785.

(24) Shieh, J. J.; Huang, R. Y. M. A pseudophase-change solution-diffusion model for pervaporation. II. Binary mixture permeation. *Sep. Sci. Technol.* **1998**, *33* (7), 933−957.

(25) Rautenbach, R.; Helmus, F. P. Some considerations on mass-transfer resistances in solution diffusion-type membrane processes. *J. Membr. Sci.* **1994**, *87* (1−2), 171−181.

(26) Heintz, A.; Stephan, W. A generalized solution diffusion-model of the pervaporation process through composite membranes 2. Concentration polarization, coupled diffusion and the influence of the porous support layer. *J. Membr. Sci.* **1994**, *89* (1−2), 153−169.

(27) Kamaruddin, H. D.; Koros, W. J. Some observations about the application of Fick's first law for membrane separation of multicomponent mixtures. *J. Membr. Sci.* **1997**, *135* (2), 147−159.

(28) Bhanushali, D.; Kloos, S.; Kurth, C.; Bhattacharyya, D. Performance of solvent-resistant membranes for non-aqueous systems: solvent permeation results and modeling. *J. Membr. Sci.* **2001**, *189* (1), 1−21.

(29) Van der Bruggen, B.; Geens, J.; Vandecasteele, C. Fluxes and rejections for nanofiltration with solvent stable polymeric membranes in water, ethanol and *n*-hexane. *Chem. Eng. Sci.* **2002**, *57* (13), 2511−2518.

(30) Bhattacharjee, S.; Chen, J. C.; Elimelech, M. Coupled model of concentration polarization and pore transport in crossflow nanofiltration. *AIChE J.* **2001**, *47* (12), 2733−2745.

(31) Van der Bruggen, B.; Vandecasteele, C. Modelling of the retention of uncharged molecules with nanofiltration. *Water Res.* **2002**, *36* (5), 1360−1368.

(32) Hagmeyer, G.; Gimbel, R. Modelling the rejection of nanofiltration membranes using zeta potential measurements. *Sep. Purif. Technol.* **1999**, *15* (1), 19−30.

(33) Garba, Y.; Taha, S.; Gondrexon, N.; Dorange, G. Ion transport modelling through nanofiltration membranes. *J. Membr. Sci.* **1999**, *160* (2), 187−200.

(34) Williams, M. E.; Hestekin, J. A.; Smothers, C. N.; Bhattacharyya, D. Separation of organic pollutants by reverse osmosis and nanofiltration membranes: Mathematical models and experimental verification. *Ind Eng. Chem. Res.* **1999**, *38* (10), 3683−3695.

(35) Bowen, W. R.; Welfoot, J. S. Modelling the performance of membrane nanofiltration - critical assessment and model development. *Chem. Eng. Sci.* **2002**, *57* (7), 1121−1137.

(36) Bowen, W. R.; Welfoot, J. S. Predictive modelling of nanofiltration: membrane specification and process optimization. *Desalination* **2002**, *147* (1−3), 197−203.

(37) de Pinho, M. N.; Semiao, V.; Geraldes, V. Integrated modeling of transport processes in fluid/nanofiltration membrane systems. *J. Membr. Sci.* **2002**, *206* (1−2), 189−200.